Epoxy Coatings Containing Nature-Inspired Antifouling Compounds Loaded in Halloysite Nanocontainers

applied sciences

MDPI

Article

Epoxy Coatings Containing Nature-Inspired Antifouling Compounds Loaded in Halloysite Nanocontainers

Daniela Pereira [1,2], Monica Tonelli [3], Joana R. Almeida [4], Marta Correia-da-Silva [2,4], Honorina Cidade [2,4,*] and Francesca Ridi [3,*]

[1] LSRE-LCM, ALiCE, Faculty of Engineering, University of Porto, Rua Dr. Roberto Frias, 4200-465 Porto, Portugal; dmvpereira@fe.up.pt
[2] Laboratory of Organic and Pharmaceutical Chemistry, Department of Chemical Sciences, Faculty of Pharmacy, University of Porto, Rua de Jorge Viterbo Ferreira n° 228, 4050-313 Porto, Portugal; m_correiadasilva@ff.up.pt
[3] Department of Chemistry "Ugo Schiff" and CSGI, University of Florence, Via della Lastruccia 3, Sesto Fiorentino, I-50019 Florence, Italy; monica.tonelli@unifi.it
[4] CIIMAR/CIMAR LA—Interdisciplinary Centre of Marine and Environmental Research, University of Porto, Terminal de Cruzeiros do Porto de Leixões, Av. General Norton de Matos s/n, 4450-208 Matosinhos, Portugal; jalmeida@ciimar.up.pt
* Correspondence: hcidade@ff.up.pt (H.C.); francesca.ridi@unifi.it (F.R.)

Abstract

Marine biofouling is a major global concern affecting the marine industry, the environment, and public health. The accumulation of organisms on submerged surfaces causes significant economic losses, including increased fuel consumption, higher pollutant emissions, and accelerated corrosion. Antifouling (AF) coatings with biocides are widely used to prevent this problem. However, many conventional biocides have been banned due to toxicity, creating an urgent need for environmentally friendly alternatives. In previous studies, we synthesized a gallic acid derivative and three flavonoids that showed AF activity against the settlement of mussel larvae (*Mytilus galloprovincialis*) together with low ecotoxicity. In the present work, to further assess their potential in marine coatings and exploit the advantages of nanocarriers in protecting and prolonging bioactive effects, these compounds were loaded into halloysite nanotubes (HNTs) and incorporated into epoxy coatings. Coatings containing the same AF compounds in free form were also prepared for comparison. HNTs were characterized by scanning electron microscopy (SEM), and compound loading was quantified by thermogravimetric (TG) analysis. The resulting composites were analyzed by SEM and dynamic water contact angle measurements. Laboratory bioassays with *M. galloprovincialis* larvae showed that coatings containing HNT-loaded synthetic compounds generally reduced larval settlement more effectively than the corresponding coatings containing the same compounds directly dispersed in the epoxy matrix, with values below 20% after both 15 and 40 h of exposure for the best-performing formulation. These findings highlight the novelty of the proposed HNT-based delivery strategy for nature-inspired synthetic antifoulants and support its potential for the development of effective and environmentally safer AF coatings.

Keywords: polyphenols; halloysite nanotubes; epoxy coating; antifouling activity

Academic Editors: Smolik Jerzy, Joanna Kacprzyńska-Gołacka and Sylwia Sowa

Received: 17 March 2026
Revised: 16 April 2026
Accepted: 21 April 2026
Published: 23 April 2026

1. Introduction

The phenomenon of attachment and colonization of fouling organisms (bacteria, algae, barnacles and shells, among others) on a variety of artificial submerged surfaces, including

ships, pipelines, and aquaculture nets, known as marine biofouling, has major economic, environmental and safety impacts [1]. The accumulation of fouling organisms on ship hulls increases the weight and surface friction resistance of the ship, leading to higher fuel consumption, thereby increasing the greenhouse gas emissions; it also promotes the corrosion of materials and increases the maintenance costs [2,3]. One of the most useful strategies to prevent marine biofouling is to protect the ship hulls with antifouling (AF) coatings. In the past, coatings based on tributyltin compounds were widely used from the 1960s until they were banned in 2008 by the International Maritime Organization because of their high toxicity for the marine environment. Alternative coatings based on copper with booster biocides have been applied; however, these compounds have also proved to have a negative impact on the marine environment, reinforcing the need for alternative, environmentally friendly solutions [4–6]. Polyphenols, including phenolic acids and flavonoids, are widely present in nature, namely, in terrestrial and marine organisms, and display a wide range of biological activities, including the potential to prevent biofouling of marine micro- and macro-organisms [7,8]. Recently, a variety of nature-inspired polyphenols obtained by chemical synthesis have shown AF activity [9,10]. A synthetic gallic acid derivative (GBA26) and three flavonoids (DH345, CC345G, and C1P) (Figure 1) were reported as potential AF agents due to their high ability to decrease, in solution, the settlement of larvae of the mussel *Mytilus galloprovincialis*, with EC_{50} values ranging from 2.34 to 16.48 µM, with high therapeutic ratios [9,11–13]. These compounds also presented very low ecotoxicity against marine non-target organisms, such as the crustacean *Artemia salina* [9,11,12] and the microalgae *Phaeodactylum tricornutum* [12]. Some of these compounds were also shown to maintain anti-settlement activity against *M. galloprovincialis* larvae after incorporation into a polyurethane-based coating [12,13]. Considering this proof-of-concept in coatings and their non-toxic profile against non-target marine species, it is therefore of interest to further investigate the possibility of preparing AF coatings with these compounds loaded in nanocarriers, a well-recognized strategy to prolong the protective effects, prevent fast releases of the antifoulants, and protect the active agents. Among all possible nanocarriers, halloysite nanotubes (HNTs) are particularly interesting in this framework, as they are biocompatible, low-cost, and non-toxic materials with distinctive adsorption properties, and their use for the preparation of filled resins and coatings is already well established in the literature [14,15]. HNTs are natural aluminosilicate tubular clays with a structural formula of $Al_2(OH)_4Si_2O_5 \cdot nH_2O$, an external diameter of about 50 nm, an inner lumen of about 15 nm, and a length of 200–2000 nm. According to the literature, HNTs have already been used to encapsulate different drugs, to modify the rate of release, to target the site of drug release, and/or to protect the drugs against aging due to chemical and enzymatic degradation [16–21]. In particular, besides their application in drug delivery, antimicrobial materials, self-healing polymeric composites, and regenerative medicine, HNTs loaded with anticorrosion agents have already been incorporated into different coatings, including polyurethane, epoxy, and polystyrene latex ones, providing an improved anticorrosion protective function [22]. Moreover, recent studies also described the use of HNTs as nanocarriers for AF compounds in the development of marine coatings, either to delay the release of such active compounds or to increase their effectiveness [23–25]. In particular, it has been demonstrated that HNTs can be used for the development of marine AF epoxy coatings containing the nanotubes loaded with either *N*-(2,4,6-trichlorophenyl) maleimide or sodium salicylate [25]. In that study, a protocol for obtaining a homogeneous dispersion of 10 wt% of HNTs within the coating was developed, and it was demonstrated that such composites can inhibit the attachment of *Vibrio natriegens* marine bacteria by preventing the release of the AF compounds. Nonetheless, only commercial AF biocides were used, and their potential negative effects towards non-target organisms were generally neglected.

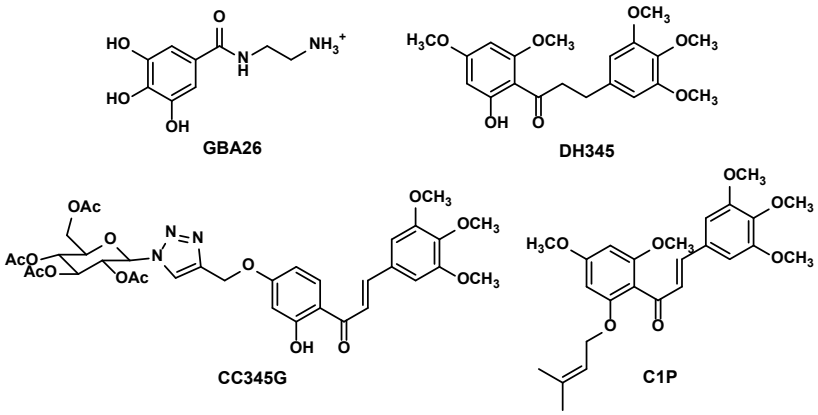

Figure 1. Structures of AF compounds loaded in HNTs.

In this work, we investigated HNTs as nanocarriers for a set of previously developed synthetic AF compounds (GBA26, DH345, CC345G, and C1P; Figure 1), which were selected because of their antifouling activity and low ecotoxicity. The novelty of the present study lies in the use of HNTs to incorporate nature-inspired, low-impact synthetic compounds into marine epoxy coatings, as an alternative to conventional biocide-based HNT systems. In some cases, HNTs were functionalized to enhance their affinity for the AF compounds and to promote their adsorption. The active compounds were either directly incorporated into marine epoxy coatings or first loaded into HNTs prior to incorporation. The physicochemical properties of the different composites were thoroughly investigated using different techniques, while the AF performance of the prepared epoxy coatings was further evaluated through settlement assays with larvae of mussel *M. galloprovincialis*.

2. Materials and Methods

2.1. Materials

Halloysite nanoclay, Dragonite (density 2.55 g/cm^3, according to the technical datasheet; length of 0.5–2 µm, according to the SEM images, specific surface area measured by means of a Coulter SA 3100 analyzer = 26 m^2/g), was obtained from Applied Minerals Inc. (Brooklyn, NY, USA). Dimethyl sulfoxide (DMSO, 0.03% water) was purchased from Merck (Darmstadt, Germany), (3-aminopropyl)triethoxysilane (APTES) was purchased from Aldrich (St. Louis, MA, USA), and NH_4OH 30% from Fluka (Seelze, Germany). The two-component epoxy coating Penguard HB red was purchased from Jotun (Sandefjord, Norway) [26]. Compounds GBA26, DH345, CC345G, and C1P were synthesized at the Laboratory of Organic and Pharmaceutical Chemistry, Faculty of Pharmacy of the University of Porto, according to previously reported procedures [9,11–13]. Artificial seawater was prepared according to Zakowski et al. [27].

2.2. Preparation of Antifouling HNTs

2.2.1. Loading of HNTs with Antifoulant GBA26

HNTs were loaded with the hydrophilic antifoulant GBA26 by adding 0.3 g of HNTs in a saturated solution of GBA26 in MilliQ water (200 mg of the compound in 5 mL of water), under magnetic stirring. Loading was promoted by applying three vacuum/air cycles, following a procedure already reported for the loading of active molecules into HNTs. This approach, based on alternating 1 h at atmospheric pressure and 1 h under vacuum (pressure < 10 mbar), was adopted to facilitate the penetration of the solution into the HNT lumen while ensuring reproducible loading conditions [25]. After the loading, the dispersion was centrifuged at 9000 rpm for 5 min, the water solution was removed, and the loaded HNTs were dried at 60 °C overnight.

2.2.2. Functionalization of HNTs with APTES

To facilitate the loading process of the other hydrophobic AF molecules, the HNT surface was functionalized with APTES, following a procedure already reported in the literature [28–30]. Briefly, 2 g of HNTs were suspended in 10 mL of ethanol in a 50 mL round-bottom flask. The suspension was kept under stirring under a nitrogen atmosphere, and APTES (250 µL) and 30% NH_4OH were added dropwise until pH 9. The reaction was kept under stirring at room temperature overnight, centrifuged for 5 min at 9000 rpm, and washed twice with 10 mL of ethanol. Finally, the centrifuged functionalized HNTs were dried for 1 day at 60 °C.

2.2.3. Loading of Functionalized HNTs with Antifoulants DH345, CC345G, and C1P

Functionalized HNTs (0.3 g) were suspended in a saturated solution of hydrophobic antifoulants in DMSO (200 mg of compounds in 6 mL of DMSO) under magnetic stirring. Loading was performed through repeated vacuum/air cycles following the procedure described in Section 2.2.1. and thoroughly detailed elsewhere [25]. After the three cycles of vacuum/air, the samples were centrifuged at 9000 rpm for 5 min, the DMSO was removed, and the loaded HNTs were dried overnight at 120 °C in a nitrogen atmosphere.

2.3. Preparation of the Composites

The epoxy coating Penguard HB is composed of two components: Comp A (epoxy resin) and Comp B (amide-based curing agent). Coatings were prepared by mixing the two components (Comp A and Comp B) at a 4:1 volume ratio, following the technical data sheet. When present, HNTs were incorporated into Comp A to achieve a weight percentage of 10% of nanotubes in the final composite. The final percentage of HNTs in the epoxy coating was selected based on previously published work [25]. HNTs were mechanically mixed with a spatula for 5 min, with a vortex for 3 min, and sonicated for 30 min at 30 °C and 59 Hz. This procedure was repeated 5 times to achieve a homogeneous dispersion of HNTs in Comp A. Then, Comp B was added, and the coating was once more mechanically mixed for 5 min with a spatula and for 3 min with a vortex, and sonicated for 30 min. The prepared coatings were both brushed onto acrylic 24-well plates and spread on smooth plastic sheets (Figure 2). Coatings were air cured and characterized after drying as described in Section 2.5. For comparison, coatings containing free AFs were also prepared by directly incorporating compounds GBA26, DH345, CC345G, and C1P into the epoxy Penguard HB, using the same concentrations of AFs that were loaded in the nanotubes. An abbreviated notation is used throughout this paper to refer to the prepared composites containing loaded nanotubes or free AF compounds, as reported in Table 1.

Figure 2. Acrylic 24-well plate brushed with prepared coatings.

Table 1. Composition of the samples prepared in this work. The percentages are calculated on the total weight.

Sample Name	HNT (%)	Free Antifoulants (%)	Coating Content
C	-	-	-
C-H	10	0	HNTs
C-FH	10	0	Functionalized HNTs
C-H-GBA26	10	0	HNTs loaded with GBA26
C-FH-DH345	10	0	Functionalized HNTs loaded with DH345
C-FH-CC345G	10	0	Functionalized HNTs loaded with CC345G
C-FH-C1P	10	0	Functionalized HNTs loaded with C1P
C-GBA26	0	0.9	GBA26
C-DH345	0	0.2	DH345
C-CC345G	0	0.3	CC345G
C-C1P	0	0.2	C1P

HNT: Halloysite nanotubes; C: pristine epoxy coating; C-H: coating with HNTs; C-FH: coating with functionalized HNTs; C-H-GBA26: coating with compound GBA26 loaded into HNTs; C-FH-DH345: coating with compound DH345 loaded into functionalized HNTs; C-FH-CC345G: coating with compound CC345G loaded into functionalized HNTs; C-FH-C1P: coating with compound C1P loaded into functionalized HNTs; C-GBA26: coating with free compound GBA26; C-DH345: coating with free compound DH345; C-CC345G: coating with free compound CC345G; C-C1P: coating with free compound C1P.

2.4. Characterization of the Nanotubes

Scanning electron microscopy (SEM) of the nanotubes was performed on a ΣIGMA Field Emission SEM (Carl Zeiss Microscopy GmbH, Jena, Germany), using an InLens detector, with an accelerating potential of 2 kV and a working distance of ~4 mm.

Fourier Transform Infrared Spectroscopy (FTIR) spectra were collected using a Cary 670 FTIR instrument (Agilent Technologies, Santa Clara, CA, USA), in transmittance mode, acquiring 128 scans for each measurement, in the spectral range of 4000–400 cm^{-1}, with a spectral resolution of 2 cm^{-1}, and a delay time of 30 s. The analyses were performed using the KBr pellet method, using 100 mg of a KBr pellet containing 1% of HNTs. Background spectra were also collected and subtracted from the spectra acquired for the samples.

Thermogravimetric (TG) analysis of pristine HNTs, functionalized HNTs, and loaded HNTs was conducted on a SDT Q600 (TA Instruments, Philadelphia, PA, USA) in a N_2 atmosphere (flow rate 100 mL/min) from room temperature to 1000 °C at 10 °C/min. TG was also performed on the pure antifoulants for comparison, using the same experimental conditions. The amount of loaded AF compounds was measured from the TG curves.

X-ray diffraction (XRD) data were collected with a XRD Dynamic 500 (Anton Paar, Graz, Austria), using as X-ray source the Cu Kα radiation (λ = 1.542 Å), at 40 kV and 49 mA, a 2θ range of 10–70°, 0.03° step size, and under spinning conditions.

Raman analyses were performed on a Renishaw inVia Qontor confocal MicroRaman system (Renishaw, Pliezhausen, Germany) equipped with a 785 nm laser, front illuminated CCD camera (256 × 1024 pixels), and a research-grade Leica DM 2700 microscope. Powder samples were placed on a glass slide, and the spectra were acquired with a 5× objective.

2.5. Characterization of the Composites

Scanning electron microscopy (SEM) of the composites was performed on a ΣIGMA Field Emission SEM (Carl Zeiss Microscopy GmbH, Jena, Germany), using an InLens detector, with an accelerating potential of 0.5 kV and a working distance of ~3 mm.

Dynamic contact angles of water were studied using a K100 Force Tensiometer (Krüss GmbH, Hamburg, Germany). Two specimens were tested for each composite by measuring the advancing and receding contact angles of the films immersed in MilliQ water at 25 °C. All films were immersed and withdrawn for 6 consecutive cycles, using a minimum and maximum immersion depths of 1 and 5 mm, respectively, at a speed of 1 mm.min^{-1}. Contact angle values were estimated through the Krüss Laboratory Desktop software (version 3.2) as the results of a linear regression of the force versus position graph. The regression was calculated in the linear region of the graph for each cycle (both advancing and receding), considering the width and thickness of the films. Data are reported as mean values ± standard deviations over all the cycles.

The amount of released GBA26 hydrophilic compound from the C-GBA26 and C-H-GBA26 composites was quantified by means of UV spectroscopy. First, a calibration curve was measured at 300 nm for GBA26 in artificial seawater (Abs = 0.007·c − 0.029, where c is the concentration of GBA26 expressed as μM). Then, films of the C-GBA26 and C-H-GBA26 composites (about 1 cm^2) were added to 5 mL of artificial seawater, continuously stirred (600 rpm) and kept at 25 °C. At predetermined times, 50 μL of suspension was withdrawn and replaced with 50 μL of artificial seawater. The withdrawal was diluted with 450 μL of artificial seawater and analyzed by UV–vis spectroscopy to quantify the amount of released GBA26 with a Cary3500 (Agilent, Santa Clara, CA, USA) in the range 190–800 nm, using quartz cuvettes, with an integration time of 0.5 s and a bandwidth of 1 nm. Aliquots withdrawn from sample C were diluted following the same procedure used for the other samples and used as a reference to remove any possible contribution arising from the coating.

2.6. Anti-Settlement Assay Against the Mussel Mytilus galloprovincialis

For the anti-settlement evaluation, *M. galloprovincialis* plantigrades were collected at Memoria beach (N 41°13′51.5″, W 8°43′15.5″) during low tide. In the laboratory, competent plantigrades exhibiting exploring behavior were selected and transferred to the coated wells. Each well was filled with filtered and sterilized natural seawater to minimize potential interferents. Coatings were tested in quadruplicate (four wells), with five plantigrades per well. A negative control (pristine coating system) was included. After 15 and 40 h, larval settlement was determined based on the presence or absence of efficiently attached byssal threads produced by each mussel larva under the tested conditions.

2.7. Statistical Analysis

One-way analysis of variance (ANOVA) was used to analyze datasets from the anti-settlement bioassay, followed by a multi-comparison Dunnett's test against the negative control ($p < 0.05$). Significance was considered at $p < 0.05$, and 95 % lower and upper confidence limits (95 %LCL; UCL). The software IBM SPSS Statistics 31 was used for statistical analysis.

3. Results and Discussion

3.1. Characterization of Pristine HNTs and Functionalized HNTs (HNTs-APTES)

The preparation of HNTs (SEM image of the nanotubes shown in Figure 3A) loaded with antifoulants and their subsequent incorporation into epoxy coatings involved multiple steps. GBA26 was loaded into HNTs. For compounds DH345, CC345G, and C1P,

the surface of HNTs was first functionalized with APTES to enhance their interaction with these hydrophobic molecules. Indeed, due to the inherent hydrophilicity of HNTs, strongly hydrophobic compounds cannot be efficiently adsorbed; therefore, surface modification of these clays with an organosilane is a promising approach to modify the surface chemistry [29] and to enable the use of HNTs as nanocarriers for hydrophobic flavonoids. Importantly, according to the literature, APTES functionalization does not compromise the biocompatibility of the nanotubes [31]. Moreover, XRD analyses also revealed the expected pattern for the nanotubes and confirmed that the functionalization with organosilane did not affect the nanotubes' structure, as previously reported in the literature [32,33] (Figure S1 in the Supplementary Materials). The FTIR spectra of pristine and functionalized HNTs, collected to confirm surface modification, are reported in Figure 3B. The presence of the small peak at 2930 cm^{-1}, attributed to C-H stretching from CH_2 groups, along with the intensification of the large band in the 3200–3500 cm^{-1} range, corresponding to N-H stretching of the NH_2 group, indicates successful APTES functionalization. It should be emphasized that the observed spectral variations in the FTIR, although small, are indeed significant. Because functionalization affects only the outer surface of the clay particles, whereas FTIR measurements reflect the response of the bulk material as a whole, the signals arising from surface-bound species are expected to be weak.

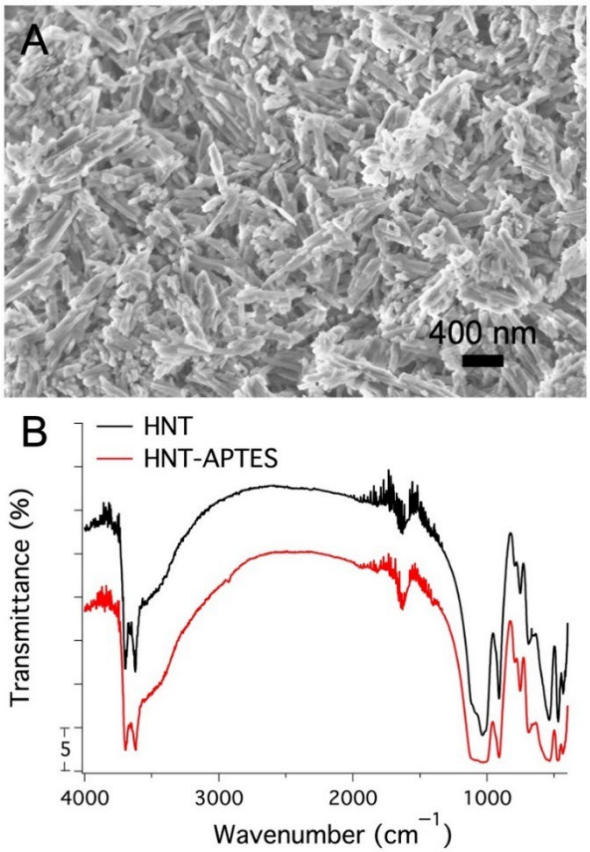

Figure 3. (**A**) SEM images of the pristine HNTs, and (**B**) FTIR spectra of pristine HNTs and functionalized nanotubes (HNT-APTES).

HNT and HNT-APTES powders were also characterized by means of Raman spectroscopy (Figure S2 in the Supplementary Materials). In agreement with the FTIR characterization, a weak but significant peak is observed for the HNT-APTES specimen in the 2850–2950 cm^{-1} range, which is fully compatible with APTES CH stretching modes.

3.2. Loading of AF Compounds in HNTs

As anticipated in Sections 2.2.1 and 2.2.3, saturated solutions of active compounds were prepared using water as the solvent for loading GBA26 in pristine HNTs, and DMSO for loading DH345, CC345G, and C1P into functionalized HNTs (HNTs-APTES), since these compounds were not soluble in water due to their non-polar nature. For successful adsorption of active molecules onto the surface of HNTs, it is important to employ a solvent in which the compounds are soluble. According to the results obtained from TG experiments (Figures S4–S13 in the Supplementary Materials and Table 2), large amounts of GBA26 were efficiently loaded into HNTs, confirming that, in this case, it was appropriate to use pristine HNTs. In the case of compounds DH345, CC345G, and C1P, the loading was less efficient (Table 2), even using functionalized HNTs. Nevertheless, considering the high AF activity of the selected compounds against the mussel *M. galloprovincialis* (EC_{50} values ranging from 2.34 and 16.48 μM) [9,11,12], the obtained loading levels were considered adequate for their application in the preparation of protective AF coatings, as further supported by the AF assays reported below.

Table 2. Amount of loaded compounds calculated from thermogravimetric (TG) curves by comparing the residual mass at 1000 °C.

Nanotubes	Loading %
HNTs with GBA26	9.3
HNTs-APTES with DH345	2.4
HNTs-APTES with CC345G	2.9
HNTs-APTES with C1P	1.6

HNTs: Halloysite nanotubes; APTES: (3-aminopropyl)triethoxysilane.

All HNTs loaded with AF compounds were also characterized by confocal Raman spectroscopy to investigate the incorporation of the compounds into the nanotubes and to evaluate possible interactions between the active molecules and the HNTs (Figure S14 in the Supplementary Materials). According to the results, the presence of the AF compounds loaded into the nanotubes modified their spectroscopic behavior. The main difference lies in the appearance of a signal at approximately 1630 cm^{-1} in the spectra, indicating the presence of the compounds and being ascribed to C=C bonds.

The HNTs loaded with the AF compounds, as well as the pristine HNTs and the functionalized HNTs, were incorporated into the epoxy coating, and the composites were characterized to evaluate their physico-chemical and AF properties. Previous studies have reported that the incorporation of different amounts of HNTs loaded with antifoulants can achieve AF activity in composites, including 10 wt% [25], 22 wt% [24], or 28 wt% [23]. Considering that using lower HNT content reduces formulation costs and decreases the consumption of the costly AF compounds, we selected 10 wt% of HNTs for incorporation into the epoxy coating. For comparison, analogous samples were also prepared by directly adding the AF compounds to the coating, using the same concentrations as those present in the coatings prepared with loaded HNTs (0.16–0.93%wt).

3.3. Characterization of the Composites

The composites were first characterized in terms of morphology and wettability. To assess the homogeneity of HNT dispersions and to discard the formation of agglomerates and clusters, the composites were initially inspected visually during mixing to ensure the obtainment of a homogeneous dispersion, and subsequently analyzed by SEM to ensure that no aggregates were present in the final dried coating. Figure S3 in the Supplementary

Materials shows the morphology of all samples investigated. According to the results, all samples display similar morphology, and no agglomerates of HNTs were found when inspecting the samples' surface, suggesting that the nanotubes are well dispersed in the coating, since HNTs' clusters would have dimensions of tens of micrometers [34].

The wettability of the prepared surfaces was also evaluated through advancing and receding contact angle measurements, as these properties are of primary importance for coatings intended for marine applications. The results (Table 3) confirmed that surface wettability was only slightly changed by the incorporation of HNTs, whether functionalized or not, and regardless of loading, in agreement with previous reports for analogous systems [25]. In particular, advancing contact angles were consistent across all samples, while differences were observed in receding angles (composites had lower values than pristine coating). As widely recognized, receding contact angles are strongly influenced by the presence of polar, hydrophilic substances and can also be affected by surface roughness [35,36]. The slight variations observed in receding contact angles can therefore be attributed to the introduction of hydrophilic moieties on the surface by the HNTs. Nevertheless, the overall wettability remained essentially unchanged, as demonstrated by the unchanged values of advancing angle and large hysteresis, supporting the suitability of these systems as protective marine coatings.

Table 3. Dynamic water contact angles obtained for the samples.

Sample	Advancing Contact Angle (°)	Receding Contact Angle (°)	Hysteresis (°)
C	95 ± 1	36 ± 3	59 ± 4
C-H	94 ± 4	28 ± 4	66 ± 8
C-FH	91 ± 4	23 ± 6	68 ± 10
C-H-GBA26	90 ± 2	25 ± 3	65 ± 5
C-FH-DH345	93 ± 3	22 ± 2	71 ± 5
C-FH-CC345G	92 ± 2	23 ± 9	69 ± 11
C-FH-C1P	93 ± 3	30 ± 9	63 ± 12

C: pristine coating; C-H: coating with HNTs; C-FH: coating with functionalized HNTs; C-H-GBA26: coating with compound GBA26 loaded into HNTs; C-FH-DH345: coating with compound DH345 loaded into functionalized HNTs; C-FH-CC345G: coating with compound CC345G loaded into functionalized HNTs; C-FH-C1P: coating with compound C1P loaded into functionalized HNTs; values express average ± standard deviations.

To evaluate the potential release of the active molecules from the composites in seawater, release kinetics experiments were performed, as often reported in studies employing HNTs as drug delivery systems [22,37]. Among the investigated compounds, GBA26 was selected as a model molecule because of its relatively higher hydrophilicity and higher loading efficiency compared with the other more hydrophobic compounds (Table 1). No detectable release of GBA26 was observed in artificial seawater after 14 days of assay (C-GBA26 and C-H-GBA26 were tested), indicating that the compound remained strongly retained either inside the HNT lumen (in C-H-GBA26) and/or within the epoxy matrix (in C-GBA26 and C-H-GBA26). Considering this result, release studies on the other antifouling molecules were not further pursued, as their stronger hydrophobic character would be expected to further hinder their diffusion from the coating. Therefore, full release profiles and kinetic modeling could not be established for these systems. Notably, despite the absence of detectable release, the antifouling activity was clearly observed under the investigated conditions and was even enhanced when the compounds were loaded into HNTs, suggesting a beneficial effect of the nanotube-based formulation, possibly associated with improved surface distribution and/or interfacial activity of the active species. This suggests

that the antifouling performance is not primarily governed by bulk diffusion, but more likely by interfacial effects [38], with the nanotube-based formulation possibly improving the distribution and exposure of the active species at or near the coating surface. Such behavior may be advantageous, as the antifouling compounds remain embedded in the coating for prolonged periods, potentially extending the durability of the protective effect.

3.4. Antifouling Evaluation of Composites

All the prepared composites (Figure 4) were tested for AF efficacy at the laboratory scale using the settlement inhibition assay of mussel (*M. galloprovincialis*) larvae as the target AF species. After 40 h of exposure to the coated surfaces, results showed that although the control coatings (C, C-H and C-FH) presented some intrinsic ability to inhibit the larval settlement, coatings containing loaded AF compounds generally exhibited higher activity (Figure 4). In particular, coatings with compounds loaded into HNTs (C-H-GBA26, C-FH-DH345, C-FH-CC345G, and C-FH-C1P) presented stronger settlement inhibition compared to those where the AF compounds were directly incorporated (C-GBA26, C-DH345, C-CC345G, and C-C1P), as shown in Figure 4, further supporting the advantages of employing HNTs for antifouling applications. These findings highlight the potential of HNT-based delivery systems in the development of effective AF coatings and suggest that their beneficial effect may not simply arise from compound release. Indeed, alternative mechanisms have been widely discussed in the literature, particularly in the context of non-leaching and bioinspired antifouling surfaces, where the inhibition of fouling is mediated by interfacial effects rather than by bulk diffusion [38]. In this framework, antifouling behavior can arise from surface-associated activity of retained compounds and/or from modifications of the physico-chemical properties of the coating that affect organism adhesion. In our system, the absence of measurable release, combined with the observed antifouling activity and its enhancement upon loading into HNTs, suggests that the mechanism is likely dominated by interfacial effects rather than by bulk diffusion. The role of halloysite nanotubes may therefore be associated with improved distribution and exposure of the active compounds at or near the coating surface.

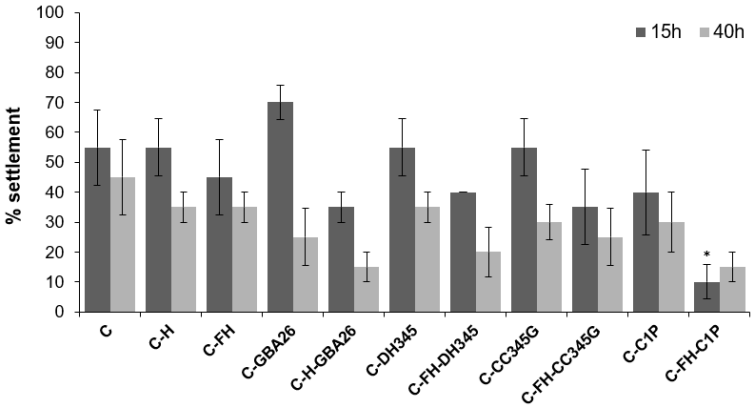

Figure 4. Efficacy of coatings with free AF compounds and with AF compounds loaded into HNTs against the settlement of mussel *M. galloprovincialis* larvae after 15 h and 40 h of exposure. Results expressed as a % of settlement of mussel larvae. C: pristine coating; C-H: coating with HNTs; C-FH: coating with functionalized HNTs; C-GBA26: coating with compound GBA26; C-H-GBA26: coating with compound GBA26 loaded into HNTs; C-DH345: coating with compound DH345; C-FH-DH345: coating with compound DH345 loaded into functionalized HNTs; C-CC345G: coating with compound CC345G; C-FH-CC345G: coating with compound CC345G loaded into functionalized HNTs; C-C1P: coating with compound C1P; C-FH-C1P: coating with compound C1P loaded into functionalized HNTs; * indicates significant differences against the respective control ($p < 0.05$, Dunnett's test).

4. Conclusions

This study demonstrates that HNTs are effective nanocarriers for the incorporation of nature-inspired synthetic AF agents into marine epoxy coatings. In this work, four previously developed AF compounds (GBA26, DH345, CC345G, and C1P) were successfully incorporated either directly into the coating matrix or after loading into HNTs, using pristine nanotubes for the gallic acid derivative (GBA26) and organosilane-functionalized HNTs for the more hydrophobic flavonoids (DH345, CC345G, and C1P), to improve their affinity for the nanotube surface. This strategy enabled efficient compound incorporation while preserving the physico-chemical properties of the coatings.

The resulting composites showed homogeneous filler dispersion within the epoxy matrix and retained the wettability characteristics of the reference coating, indicating that HNT incorporation does not adversely affect the surface behavior of the protective system. Release experiments performed on GBA26, selected as the most hydrophilic and highly loaded compound, showed no detectable release into the aqueous medium, suggesting strong retention of the active molecules within the nanotubes and/or the epoxy matrix. This feature may be advantageous for prolonging coating efficacy while limiting rapid and uncontrolled release into the marine environment.

Laboratory bioassays with *M. galloprovincialis* larvae demonstrated that HNT-loaded polyphenols enhance the anti-settlement performance of epoxy coatings compared with the direct incorporation of the free compounds. Although the control coatings already exhibited some intrinsic inhibition of larval settlement, the presence of AF molecules generally improved the biological response, and the HNT-based formulations outperformed the corresponding coatings containing the same amount of freely dispersed compounds. These findings support the role of HNTs as functional carriers capable of improving the effectiveness of the active agents.

Among the tested formulations, C-FH-C1P showed the best overall performance, with the lowest larval settlement at both exposure times, indicating the strongest and most persistent anti-settlement effect. This behavior does not appear to be simply related to a higher loading amount, but rather to a more favorable balance between molecular activity, affinity for the carrier, and availability at the coating/seawater interface. In line with the non-leaching behavior observed for these systems, this result further supports the hypothesis that antifouling performance is mainly governed by interfacial effects rather than by bulk diffusion, with HNTs likely contributing to optimize the distribution and exposure of the active compound at or near the coating surface.

Overall, the results indicate that the use of HNT-based nanocarriers is a promising strategy for improving the performance of epoxy AF coatings and for optimizing the use of synthetic nature-inspired AF agents. Such systems may be of interest for the protection of submerged marine surfaces, where prevention of early-stage fouling, prolonged coating efficacy, and reduced release of active agents are highly desirable.

Supplementary Materials: The following supporting information can be downloaded at: https://www.mdpi.com/article/10.3390/app16094114/s1, Figure S1: XRD diffractograms of pristine HNTs and HNTs functionalized with APTES; Figure S2: Raman spectra of pristine HNTs and HNTs functionalized with APTES; Figure S3: SEM images of the investigated samples; Figure S4: Thermogravimetric (TG) analysis of HNTs Dragonite; Figure S5: TG analysis of HNTs Dragonite functionalized with APTES; Figure S6: TG analysis of compound GBA26; Figure S7: TG analysis of compound GBA26 loaded in HNTs Dragonite; Figure S8: TG analysis of compound DH345; Figure S9: TG analysis of compound DH345 loaded in HNTs functionalized with APTES; Figure S10: TG analysis of compound CC345G; Figure S11: TG analysis of compound CC345G loaded in HNTs functionalized with APTES; Figure S12: TG analysis of compound C1P; Figure S13: TG analysis of compound C1P loaded in HNTs functionalized with APTES; Figure S14: Raman spectra of the

synthesized active molecules together with HNTs and HNTs loaded with the AF compounds: (A) compound GBA26, HNT, and HNT loaded with GBA26, (B) compound DH345, HNT-APTES, and HNT-APTES loaded with DH345, (C) compound CC345G, HNT-APTES, and HNT-APTES loaded with CC345G, and (D) compound C1P, HNT-APTES, and HNT-APTES loaded with C1P.

Author Contributions: Conceptualization, D.P., H.C. and F.R.; methodology, J.R.A. and F.R.; validation, D.P., M.T., J.R.A., H.C. and F.R.; formal analysis, D.P., M.T., J.R.A., M.C.-d.-S., H.C. and F.R.; investigation, D.P. and M.T.; resources, J.R.A., M.C.-d.-S., H.C. and F.R.; data curation, D.P. and M.T.; writing—original draft preparation, D.P.; writing—review and editing, D.P., M.T., J.R.A., M.C.-d.-S., H.C. and F.R.; supervision, H.C. and F.R.; project administration, M.C.-d.-S. and F.R.; funding acquisition, M.C.-d.-S. and F.R. All authors have read and agreed to the published version of the manuscript.

Funding: This research was funded by CSGI (Consorzio Interuniversitario per lo Sviluppo dei Sistemi a Grande Interfase) and MIUR-Italy ("Progetto Dipartimenti di Eccellenza 2018–2022" and "Dipartimenti di Eccellenza 2023–2027 DICUS 2.0" allocated to Department of Chemistry "Ugo Schiff", University of Florence). The research was also funded under the "Dalla ricerca all'impresa"—Call for tender No. 341 of 15/03/2022 of Italian Ministry of Research funded by the European Union—NextGenerationEU, CUP: B83C22004890007, Project title "3A-ITALY—Made-in-Italy circolare e sostenibile". This research was also funded by national funds through FCT—Fundação para a Ciência e a Tecnologia, I.P., and by the European Commission's Recovery and Resilience Facility, within the scope of UID/04423/2025 (https://doi.org/10.54499/UID/04423/2025), UID/PRR/04423/2025 (https://doi.org/10.54499/UID/PRR/04423/2025), and LA/P/0101/2020 (https://doi.org/10.54499/LA/P/0101/2020). This work was also supported by the projects nr 17414 and 17136 (COMPETE2030-FEDER-01194000 and COMPETE2030-FEDER-00853900), funded by COMPETE2030 and PORTUGAL2030. D.P. and J.R.A. acknowledge FCT (PhD grant SFRH/BD/147207/2019) and work contract (https://doi.org/10.54499/2022.03876.CEECIND/CP1728/CT0005) under the Scientific Employment Stimulus Individual Call, respectively.

Institutional Review Board Statement: Not applicable.

Informed Consent Statement: Not applicable.

Data Availability Statement: The original contributions presented in this study are included in the article/Supplementary Materials. Further inquiries can be directed to the corresponding authors.

Conflicts of Interest: The authors declare no conflicts of interest.

Abbreviations

The following abbreviations are used in this manuscript:

AF	Antifouling
APTES	(3-aminopropyl)triethoxysilane
FTIR	Fourier transform infrared spectroscopy
HNTs	Halloysite nanotubes
SEM	Scanning electron microscopy
TG	Thermogravimetric

References

1. Hadžić, N.; Jovanović, I.; Vladimir, N. Biofouling of ships and offshore structures: Research trends and future pathways. *Ocean Eng.* **2026**, *347*, 123988. [CrossRef]
2. Gu, Y.; Yu, L.; Mou, J.; Wu, D.; Xu, M.; Zhou, P.; Ren, Y. Research Strategies to Develop Environmentally Friendly Marine Antifouling Coatings. *Mar. Drugs* **2020**, *18*, 371. [CrossRef] [PubMed]
3. Liu, D.; Shu, H.; Zhou, J.; Bai, X.; Cao, P. Research Progress on New Environmentally Friendly Antifouling Coatings in Marine Settings: A Review. *Biomimetics* **2023**, *8*, 200. [CrossRef] [PubMed]
4. Gomez-Banderas, J. Marine Natural Products: A Promising Source of Environmentally Friendly Antifouling Agents for the Maritime Industries. *Front. Mar. Sci.* **2022**, *9*, 858757. [CrossRef]

5. Perina, F.C.; Abessa, D.M.d.S.; Pinho, G.L.L.; Castro, Í.B.; Fillmann, G. Toxicity of antifouling biocides on planktonic and benthic neotropical species. *Environ. Sci. Pollut. Res.* **2023**, *30*, 61888–61903. [CrossRef]
6. Weber, F.; Esmaeili, N. Marine biofouling and the role of biocidal coatings in balancing environmental impacts. *Biofouling* **2023**, *39*, 661–681. [CrossRef]
7. Zhang, T.-Y.; Wang, K.-Y.; Chen, J.-Y.; Zheng, R.; Li, H.-J.; Wu, Y.-C. Flavonoid Natural Products as Potential Green Antifoulants for Marine Composite Coatings. *Chem. Biodivers.* **2026**, *23*, e03710. [CrossRef]
8. Zhao, W.; Wu, Z.; Liu, Y.; Dai, P.; Hai, G.; Liu, F.; Shang, Y.; Cao, Z.; Yang, W. Research Progress of Natural Products and Their Derivatives in Marine Antifouling. *Materials* **2023**, *16*, 6190. [CrossRef]
9. Pereira, D.; Gonçalves, C.; Martins, B.T.; Palmeira, A.; Vasconcelos, V.; Pinto, M.; Almeida, J.R.; Correia-Da-Silva, M.; Cidade, H. Flavonoid Glycosides with a Triazole Moiety for Marine Antifouling Applications: Synthesis and Biological Activity Evaluation. *Mar. Drugs* **2021**, *19*, 5. [CrossRef]
10. Wang, X.; Jiang, X.; Yu, L. Preparation and evaluation of polyphenol derivatives as potent antifouling agents: Addition of a side chain affects the biological activity of polyphenols. *Biofouling* **2022**, *38*, 29–41. [CrossRef]
11. Almeida, J.R.; Moreira, J.; Pereira, D.; Pereira, S.; Antunes, J.; Palmeira, A.; Vasconcelos, V.; Pinto, M.; Correia-da-Silva, M.; Cidade, H. Potential of synthetic chalcone derivatives to prevent marine biofouling. *Sci. Total Environ.* **2018**, *643*, 98–106. [CrossRef]
12. Neves, A.R.; Vilas Boas, C.; Gonçalves, C.; Vasconcelos, V.; Pinto, M.; Silva, E.R.; Sousa, E.; Almeida, J.R.; Correia-da-Silva, M. Gallic acid derivatives as inhibitors of mussel (*Mytilus galloprovincialis*) larval settlement: Lead optimization, biological evaluation and use in antifouling coatings. *Bioorg. Chem.* **2022**, *126*, 105911. [CrossRef]
13. Pereira, D.; Lima, É.; Correia, D.; Vasconcelos, V.; Pinto, M.; Correia-Da-Silva, M.; Almeida, J.R.; Cidade, H. Dihydrochalcone derivatives as promising antifoulants: Synthesis, bioactivity evaluation and performance in coatings. *Biofouling* **2025**, *41*, 798–808. [CrossRef] [PubMed]
14. Buyondo, K.A.; Kasedde, H.; Kirabira, J.B. A comprehensive review on kaolin as pigment for paint and coating: Recent trends of chemical-based paints, their environmental impacts and regulation. *Case Stud. Chem. Environ. Eng.* **2022**, *6*, 100244. [CrossRef]
15. Rawtani, D.; Agrawal, Y. Multifarious applications of halloysite nanotubes: A review. *Rev. Adv. Mater. Sci* **2012**, *30*, 282–295.
16. Biddeci, G.; Spinelli, G.; Colomba, P.; Di Blasi, F. Nanomaterials: A Review about Halloysite Nanotubes, Properties, and Application in the Biological Field. *Int. J. Mol. Sci.* **2022**, *23*, 11518. [CrossRef]
17. Massaro, M.; Cavallaro, G.; Colletti, C.G.; Lazzara, G.; Milioto, S.; Noto, R.; Riela, S. Chemical modification of halloysite nanotubes for controlled loading and release. *J. Mater. Chem. B* **2018**, *6*, 3415–3433. [CrossRef]
18. Massaro, M.; Lazzara, G.; Noto, R.; Riela, S. Halloysite nanotubes: A green resource for materials and life sciences. *Rend. Lincei Sci. Fis. Nat.* **2020**, *31*, 213–221. [CrossRef]
19. Yuan, P.; Tan, D.; Annabi-Bergaya, F. Properties and applications of halloysite nanotubes: Recent research advances and future prospects. *Appl. Clay Sci.* **2015**, *112–113*, 75–93. [CrossRef]
20. Abdullayev, E.; Lvov, Y. Halloysite clay nanotubes for controlled release of protective agents. *J. Nanosci. Nanotechnol.* **2011**, *11*, 10007–10026. [CrossRef]
21. Lvov, Y.M.; Shchukin, D.G.; Möhwald, H.; Price, R.R. Halloysite Clay Nanotubes for Controlled Release of Protective Agents. *ACS Nano* **2008**, *2*, 814–820. [CrossRef] [PubMed]
22. Lvov, Y.; Wang, W.; Zhang, L.; Fakhrullin, R. Halloysite Clay Nanotubes for Loading and Sustained Release of Functional Compounds. *Adv. Mater.* **2016**, *28*, 1227–1250. [CrossRef] [PubMed]
23. Fu, Y.; Gong, C.; Wang, W.; Zhang, L.; Ivanov, E.; Lvov, Y. Antifouling Thermoplastic Composites with Maleimide Encapsulated in Clay Nanotubes. *ACS Appl. Mater. Interfaces* **2017**, *9*, 30083–30091. [CrossRef] [PubMed]
24. Fu, Y.; Wang, W.; Zhang, L.; Vinokurov, V.; Stavitskaya, A.; Lvov, Y. Development of Marine Antifouling Epoxy Coating Enhanced with Clay Nanotubes. *Materials* **2019**, *12*, 4195. [CrossRef]
25. Tonelli, M.; Perini, I.; Ridi, F.; Baglioni, P. Improving the properties of antifouling hybrid composites: The use of Halloysites as nano-containers in epoxy coatings. *Colloids Surf. A Physicochem. Eng. Asp.* **2021**, *623*, 126779. [CrossRef]
26. JOTUN. Technical Data Sheet Penguard HB. Available online: https://www.jotun.com/ww-en/industries/products/penguard-hb-ii (accessed on 9 January 2026).
27. Zakowski, K.; Narozny, M.; Szocinski, M.; Darowicki, K. Influence of water salinity on corrosion risk—The case of the southern Baltic Sea coast. *Environ. Monit. Assess.* **2014**, *186*, 4871–4879. [CrossRef]
28. Tan, D.; Yuan, P.; Liu, D.; Du, P. Chapter 8—Surface Modifications of Halloysite. In *Developments in Clay Science*; Elsevier: Amsterdam, The Netherlands, 2016; Volume 7, pp. 167–201.
29. Yuan, P.; Southon, P.D.; Liu, Z.; Green, M.E.R.; Hook, J.M.; Antill, S.J.; Kepert, C.J. Functionalization of Halloysite Clay Nanotubes by Grafting with γ-Aminopropyltriethoxysilane. *J. Phys. Chem. C* **2008**, *112*, 15742–15751. [CrossRef]
30. Yuan, P.; Southon, P.D.; Liu, Z.; Kepert, C.J. Organosilane functionalization of halloysite nanotubes for enhanced loading and controlled release. *Nanotechnology* **2012**, *23*, 375705. [CrossRef]

31. Rapacz-Kmita, A.; Foster, K.; Mikołajczyk, M.; Gajek, M.; Stodolak-Zych, E.; Dudek, M. Functionalized halloysite nanotubes as a novel efficient carrier for gentamicin. *Mater. Lett.* **2019**, *243*, 13–16. [CrossRef]
32. Abdouss, M.; Radgoudarzi, N.; Mohebali, A.; Kowsari, E.; Koosha, M.; Li, T. Fabrication of Bio-Nanocomposite Based on HNT-Methionine for Controlled Release of Phenytoin. *Polymers* **2021**, *13*, 2576. [CrossRef]
33. Falcón, J.M.; Sawczen, T.; Aoki, I.V. Dodecylamine-Loaded Halloysite Nanocontainers for Active Anticorrosion Coatings. *Front. Mater.* **2015**, *2*, 69. [CrossRef]
34. Makaremi, M.; Pasbakhsh, P.; Cavallaro, G.; Lazzara, G.; Aw, Y.K.; Lee, S.M.; Milioto, S. Effect of Morphology and Size of Halloysite Nanotubes on Functional Pectin Bionanocomposites for Food Packaging Applications. *ACS Appl. Mater. Interfaces* **2017**, *9*, 17476–17488. [CrossRef]
35. Rupp, F.; Scheideler, L.; Geis-Gerstorfer, J. Effect of Heterogenic Surfaces on Contact Angle Hysteresis: Dynamic Contact Angle Analysis in Material Sciences. *Chem. Eng. Technol.* **2002**, *25*, 877–882. [CrossRef]
36. Meiron, T.S.; Marmur, A.; Saguy, I.S. Contact angle measurement on rough surfaces. *J. Colloid Interface Sci.* **2004**, *274*, 637–644. [CrossRef]
37. Lisuzzo, L.; Cavallaro, G.; Milioto, S.; Lazzara, G. Halloysite Nanotubes Coated by Chitosan for the Controlled Release of Khellin. *Polymers* **2020**, *12*, 1766. [CrossRef]
38. Scardino, A.J.; de Nys, R. Mini review: Biomimetic models and bioinspired surfaces for fouling control. *Biofouling* **2011**, *27*, 73–86. [CrossRef]